JOURNAL OF Materials CHEMISTRY

Synthesis and characterization of a mordenite membrane on an α-Al_2O_3 tubular support

Adalgisa Tavolaro,*[a] Anne Julbe,[b] Christian Guizard,[b] Angelo Basile,[c] Louis Cot[b] and Enrico Drioli[a,c]

[a]*Department of Chemical Engineering and Materials, University of Calabria, I-87030 Arcavacata, Rende, Cosenza, Italy. E-mail: tavolaro@unical.it*
[b]*Laboratoire de Matériaux et Procédés Membranaires (CMRS-UMR 5635), Ecole Nationale Supérieure de Chimie, 8 Rue de l'Ecole Normale, F-34296 Montpellier Cedex 5, France*
[c]*Research Institute on Membranes and Modelling of Chemical Reactors (CNR-IRMERC), c/o Department of Chemical Engineering and Materials, University of Calabria, I-87030 Rende, Cosenza, Italy*

Received 5th January 2000, Accepted 4th February 2000
Published on the Web 30th March 2000

The present paper reports the *in situ* hydrothermal synthesis of a composite mordenite membrane. In this process, mordenite forms at the surface and within the pores of a porous ceramic alumina support by nucleation and crystallization from a mixture containing alumina and silica species. The structure and texture of the composite membrane were identified by XRD and SEM, as well as by single gas permeation at room temperature with H_2, N_2, O_2, Ar, CO, He and CH_4. The permeation resulting as a function of transmembrane pressure revealed a small viscous flow contribution for gas transport through the MOR composite membrane. Furthermore, these preliminary results (order of gas permeance and ideal selectivities) suggest that Knudsen diffusion is the dominant transport mechanism for the investigated series of gases, although an ideal selectivity slightly higher than the Knudsen selectivity was obtained, namely $\alpha = 1.6$ at $\Delta p = 0.6$ bar for CH_4/N_2.

Introduction

During the last few years, increasing attempts have been focused on developing zeolite membranes for both separations and catalytic applications. Zeolite membranes are completely different from simple crystalline zeolite powders and their synthesis requires new preparation strategies. Tavolaro and Drioli in an extensive review have recently classified zeolite membranes according to their morphology and application.[1]

In order to prepare zeolite composition membranes, zeolite crystals need to grow on porous substrates to form a continuous thin film, in which the zeolite pores are the only available pathways for the transport of gas or reactive molecules. The objective of this work was to determine the optimal experimental conditions for obtaining a composite membrane with a mordenite (MOR) structure by means of a synthesis method called multi *in situ* crystallization (MISC).[2]

Its high thermal stability and exceptionally high acid stability make MOR very important as an industrial catalyst and selective adsorbent. It is used in the separation of gases or liquids involving acid components and is extensively applied as a catalyst for hydrocarbon conversion reactions. MOR-based catalysts in various forms are used in steam reforming for hydrogen manufacture,[3] polymerization,[4] alkylation,[5] disproportionation and dehydration.[6]

MOR is difficult to prepare in the presence of a support, but it is useful for applications in the field of gas separations and catalytic membrane reactors. In this paper, we show the possibility of preparing a MOR membrane by means of the MISC synthesis method from traditional gel mixtures and of studying the crystallization of oriented zeolite layers and zeolite crystals while varying some reaction parameters.

Nishiyama *et al.*[7] and Matsukata *et al.*[8] synthesized a membrane with a MOR structure on a porous alumina support by the vapor-phase transport (VPT) method. In the VPT method an aluminosilicate dry gel crystallizes by amine or water vapors. In the present work, we report on the hydrothermal synthesis of a MOR composite membrane prepared by direct contact of the support with the gel containing all the crystallization precursors.

In an attempt to obtain a layer of oriented MOR microcrystals with elliptical channels grown perpendicularly to the surface of the support, we focused on the effect of several synthesis parameters, such as the composition of the crystallization mixture (templating agent, pH, silica source, Si/Al and Si/Na ratios) or the hydrothermal conditions (temperature and time). Another main objective of this work was to explore the possibility of using porous zeolite membranes such as catalytic membrane reactors.

The structure and texture of the composite materials were identified by XRD, SEM and single gas permeation at room temperature with H_2, N_2, O_2, Ar, CO, He and CH_4.

Experimental

For the synthesis of the MOR membrane the reactants were sodium aluminate (99%, Strem Chemicals), $Al_2(SO_4)_3 \cdot 16H_2O$ (purum, Fluka), sodium silicate (purum, Fluka), fumed silica (aerosil 380, Degussa), colloidal silica (AS-40, DuPont), tetraethylammonium hydroxide (TEAOH) (35 wt.% sol., Aldrich), tetraethylammonium bromide (TEABr) (purum, Fluka). Table 1 reports the gel compositions used.

Fig. 1 shows the preparation procedure for the mordenite composite membrane. The method comprises two stages. In the first, a gel containing silica, aluminate and the templating species is prepared by dissolving finely divided silica in an alkaline hydroxide solution. In the second stage, this mixture is used for hydrothermal treatment in the presence of the porous support. The α-Al_2O_3 tubular supports were supplied by

Table 1 Experimental conditions and materials resulting from the hydrothermal treatment of the mixture xNa$_2$O–Al$_2$O$_3$–ySiO$_2$–zTEAOH–kTEABr–jH$_2$O (x, y, z, k and j are the molar concentrations)

Sample	x	y	z	j	k	T_{synth}/K	Silica source	Zeolite structure	Morphology	Crystal size/μm
1	10.0	25.0		1250		423	Aerosil	[a]?	Single large rhomboidal crystals	50
2	3.6	43.6		1250		423	Aerosil	MOR	Prismatic crystals	13
3	5.7	30.0		1500	3.0	423	Aerosil	MOR	Polycrystalline layer	15
4	10.0	30.0		1500	3.0	423	Colloidal	MOR + Amorphous	Small porous aggregate	—
5	5.7	43.6		1250		423	Colloidal	MOR + Amorphous	Few porous aggregate	2
6	5.7	30.0	3.0	1500		423	Colloidal	MOR + Amorphous	Porous aggregate	—
7	10.0	30.0	3.0	1500		423	Colloidal	MOR	Polycrystalline layer	<2
8	11.4	43.6	3.0	1250		423	Colloidal	MOR	Polycrystalline layer	<2
9	5.7	30.0	3.0	1500		423	Colloidal	MOR	Polycrystalline layer	<2
10	10.0	30.0	3.0	1500		443	Aerosil	MOR	Polycrystalline layer	<2
11	10.0	30.0	3.0	1500		443	Colloidal	MOR	No continuous crystalline layer	—

[a]Amines were used as template agents.

Schumacher Gmbh (Germany). The single-channel, asymmetric supports were 250 or 50 mm long, the internal and external diameters amounted to 7 mm and 10 mm, respectively, and the pore width was 0.2 μm at the inner side.

The asymmetric pore system was well contacted by the synthesis mixture, because it was fully immersed in the mixture and a small pressure difference was applied to penetrate the gel into the pores and facilitate crystallization on all sides of the tube.

The hydrothermal synthesis was carried out in modified Morey-type PTFE-lined autoclaves (29.4 or 6.8 cm^3) without agitation. The autoclave was heated at 423 K or 443 K in an oven. After the hydrothermal synthesis (typically 4 to 5 days), the support was washed with distilled water and dried at 373 K before analysis.

Products were identified and their crystallinity determined by XRD with a Philips PW 1730/10 diffractometer using Cu Kα radiation. The scanning rate for crystallinity was 1.2° 2θ min^{-1}. The crystal sizes and morphologies were studied by scanning electron microscopy (FESEM, Hitachi S4500; and SEM, Leica Stereoscan S260).

More than 50 samples (about 3 cm long) were prepared from 11 different reaction mixture compositions. The reaction mixture leading to the most uniform and continuous polycrystalline layer was selected to prepare a 25 cm long composite membrane on an α-alumina support. The same synthesis was repeated 3 times on the same support before obtaining the final composite membrane.

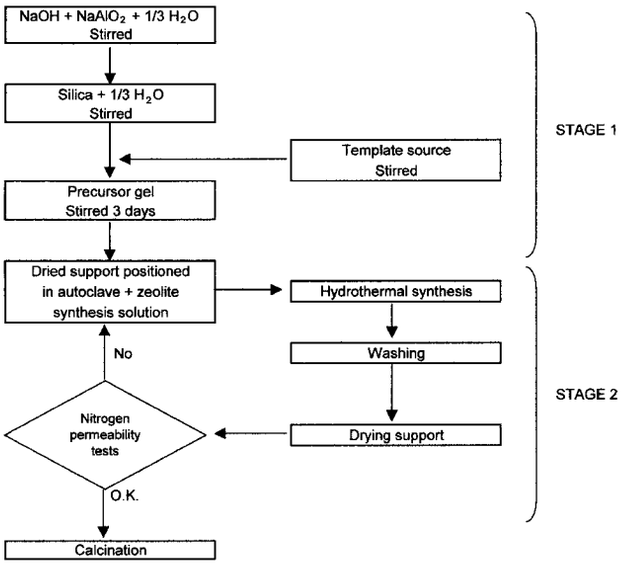

Fig. 1 Schematic illustration of the preparation of a MOR membrane by the multi *in situ* crystallization method.

The as-synthesized MOR membranes were thermally treated up to 843 K in nitrogen and in air with a heating rate of 1.0 K min^{-1}.

The experimental apparatus used for single gas permeance measurements consists of a stainless-steel module (for 25 cm long membranes), a bubble flowmeter, two manometers, and seven pure gas cylinders. The zeolite membrane was located in the stainless-steel module and equipped with four graphite rings (2.8 g each, composed of 99.53% C and 0.47% S) supplied by Gee Graphite Ltd, England. The rings ensure that the permeate and residue gases do not mix with each other in the module. Prior to the permeation measurements, the calcined

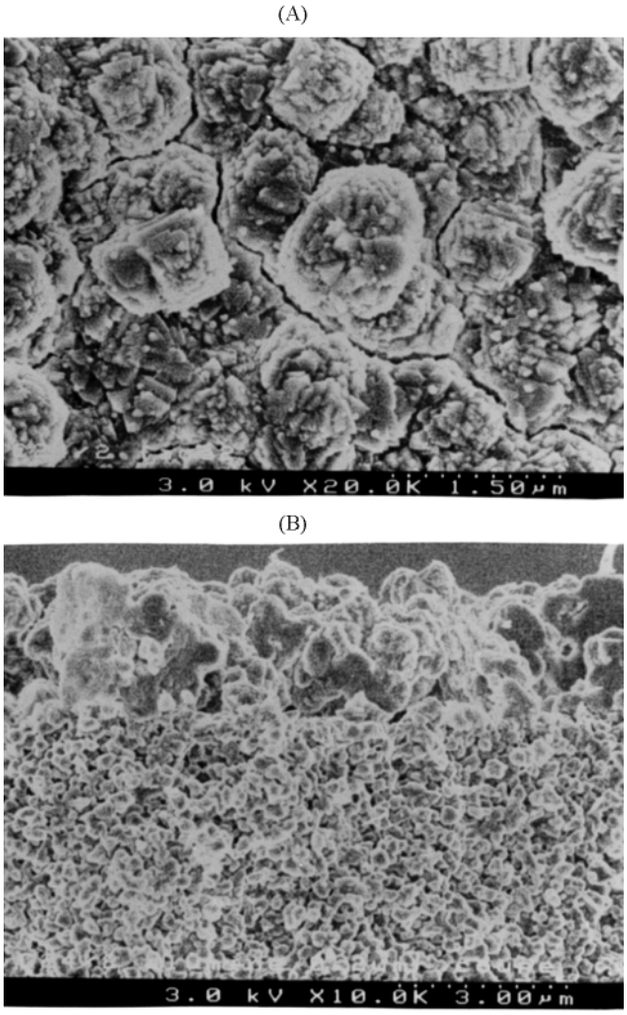

Fig. 2 SEM micrographs of the top surface (A) and cross-section (B) of sample 9.

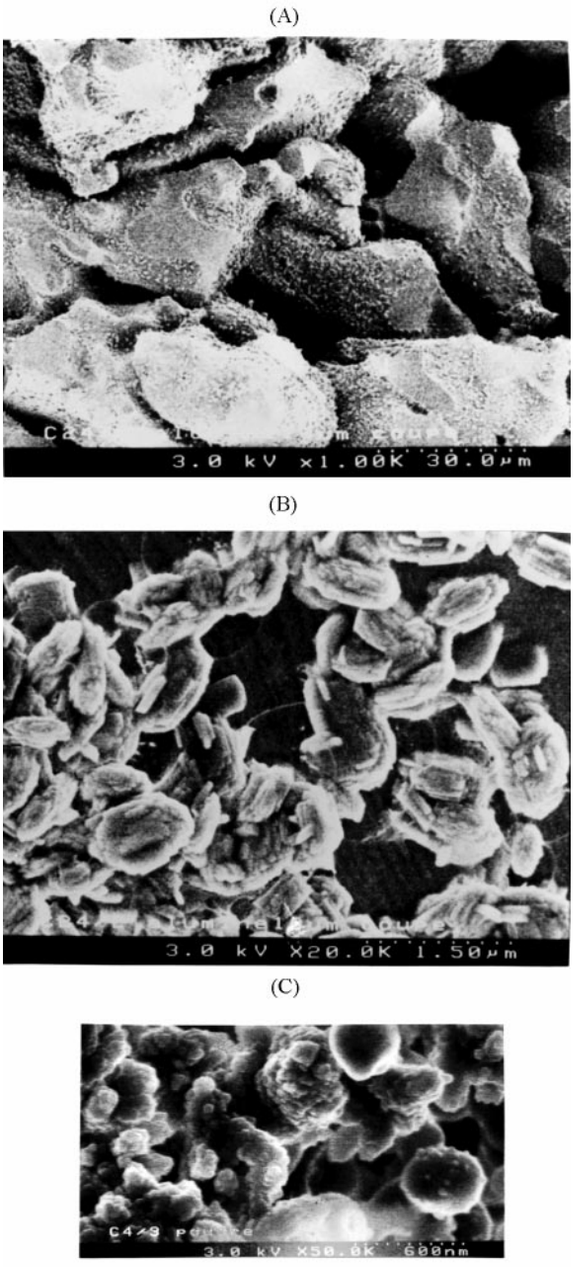

Fig. 3 SEM images of sample 9: (A) cross-section of the macroporous layer of the support, (B) MOR zeolite crystals in macroporous layer of the support and (C) section of the microporous layer of the support.

membrane was outgassed overnight at 473 K in a nitrogen flow. The permeance of pure gases (H_2, N_2, O_2, Ar, CO, He and CH_4 of purity $>99.995\%$) through the zeolite membrane were measured as a function of the transmembrane pressure (between 0.15×10^5 and 1.55×10^5 Pa) at 294 K using a bubble flowmeter. The permeate pressure in all runs was kept constant at 1 bar.

Results and discussion

Many synthesis parameters can influence the zeolite membrane characteristics (quality, morphology, crystallinity, zeolite crystalline layer structure and orientation of zeolite crystals); some factors are related to the reaction medium, while others are related to the synthesis method. The experimental conditions applied (starting precursors, compositions, and hydrothermal conditions) and the corresponding sample designations are reported in Table 1.

Structure and morphology of the synthesized membranes

The XRD patterns of the scrapped supports of the samples (2–11) were comparable to the XRD of MOR-type zeolites reported in the literature.[9] They contain the peaks related to the support but the most intense peaks correspond to well crystallized MOR ($d=4.00$; 3.47; 3.40; 3.22 Å).

The XRD patterns of the samples 4, 5 and 6 also contained an amorphous phase. Fig. 2 shows the top surface (A) and cross-section (B) of sample 9 treated at 843 K. It reveals a polycrystalline zeolitic film formed on the inner surface of the ceramic tube. The crystal morphology observed in Fig. 3 is similar to that reported in the literature for the MOR zeolite.[10] The mean size of the crystals formed on the top surface was about 500 nm and the film thickness was <2.0 µm. Cracks were also observed at the surface of the membrane. On the

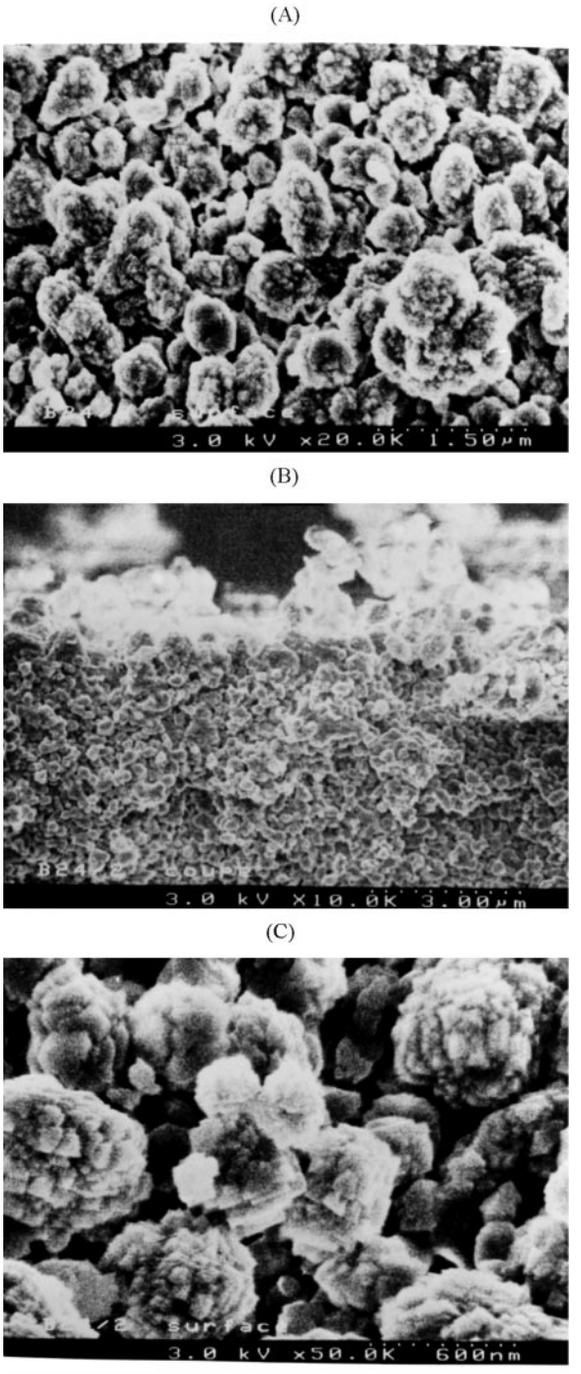

Fig. 4 SEM microphotographs of the top surface (A and B) and cross-section (C) of sample 8.

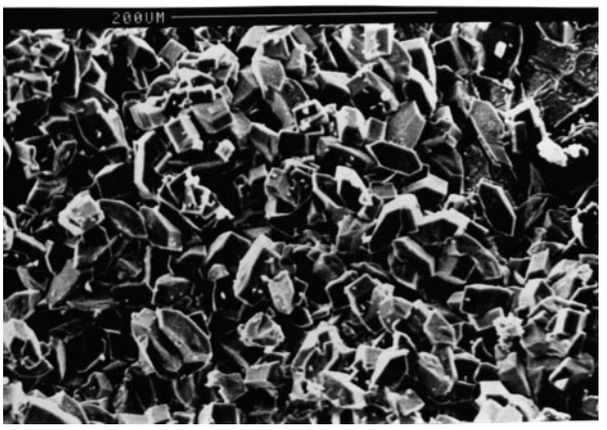

Fig. 5 SEM microphotograph of the top surface of sample 2.

other hand, the inner layers of the macroporous support were partially filled with zeolite. Indeed FESEM revealed that zeolite crystals also formed within the support (Fig. 3). Taking into account the size of the larger crystals in each layer of the support, it seems that the crystallization rate increases when pore sizes of the support decrease. As shown in Fig. 4 the first inner layer of the support has been converted to a composite MOR/α-Al_2O_3 layer. Apparently, there were no big defects in the boundary between the top and intermediate layers.

The morphology of the composite zeolite membrane 9 suggests that the crystallization started by heterogeneous nucleation at the surface of the alumina grains forming the support. The formation of intergrown crystals with no macrodefects in between is a key condition leading to a good quality membrane for gas separation applications. Figs. 4–6 show the top surfaces and cross-sections of samples 8, 2 and 3,

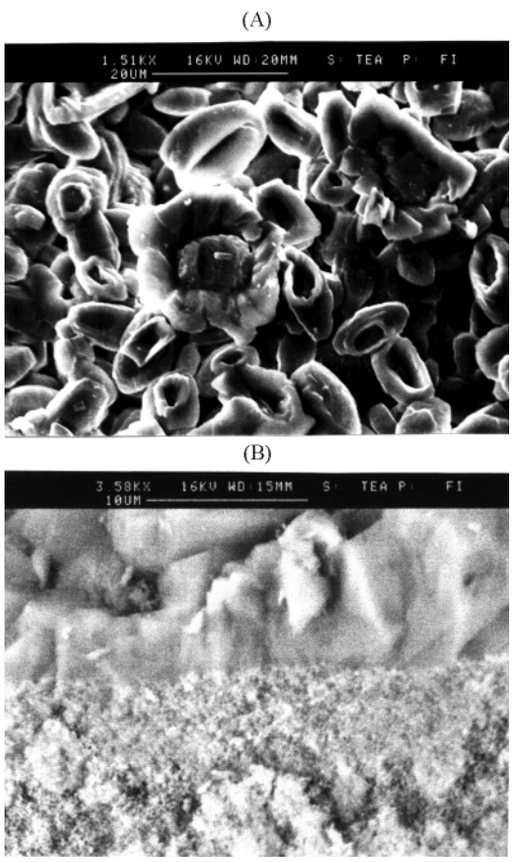

Fig. 6 SEM microphotographs of the top surface (A) and cross-section (B) of sample 3 (after ref. 1: reproduced by kind permission of *Advanced Materials*).

respectively. In the three cases, discrete (not interconnected) crystals are observed, suggesting that these MOR deposits resulted from a progressive accumulation of zeolite crystals formed by homogeneous nucleation in the liquid phase. It should be noted that MOR crystal morphologies and sizes are very different (prismatic) in the three samples. Big prismatic crystals were obtained without any template in the starting mixture (sample 2 Fig. 5), whereas rounded crystals were obtained with the TEABr or TEAOH template. The smallest crystals were obtained with the TEAOH template. When the starting mixture was too basic, the support was partially dissolved. Fig. 7 shows the cross-section for sample 7 (hydrothermal synthesis at 150 °C for 5 d).

Fig. 8 shows the morphology of sample 11 and reveals the effect of the synthesis temperature (5 d at 170 °C) on film formation. A compact layer formed at 170 °C (Fig. 8A and B), but the crystallization was irregular although crystals formed also in the macropores of the support (Fig. 8C and D). Starting from the same composition and synthesis conditions but replacing the silica source (colloidal silica) with fumed silica leads to a discontinuous MOR layer. The morphology of the corresponding sample (10) is shown in Fig. 9.

The above comments would indicate that the most attractive sample is sample 9 in which interconnected MOR zeolite crystals formed both at the surface and in the porous structure of the macroporous support. Such a membrane morphology, with a sufficient thickness of interconnected crystals could be expected to lead to a membrane with a separation performance similar to that of the MOR crystals (*i.e.*, very selective, possibility of ion exchange). The synthesis of sample 9 has been reproduced 3 times on a 25 cm long tubular support in order to evaluate the quality and transport properties of the membrane.

Single gas permeation studies

Gas permeation studies are of interest for checking the quality and evaluating the selectivity of the synthesized zeolite membrane. Classically, good quality membranes (free of macrodefects) are gas tight when their channels are still obstructed by the templating agent. If the membrane is permeable (*e.g.* to N_2) at this stage, its means that the zeolite film is discontinuous or contains microdefects (intercrystal pores in the range 5–50 nm) or macrodefects (greater than 50 nm).

The synthesized membrane was found to be gas tight before the removal of the template by calcination, indicating the absence of pinholes or cracks in the membrane equivalent to sample 9 but obtained after three consecutive hydrothermal syntheses.

After this first evaluation of membrane quality, the template was eliminated from the zeolite structure by a calcination treatment at 843 K. This thermal treatment was carried out

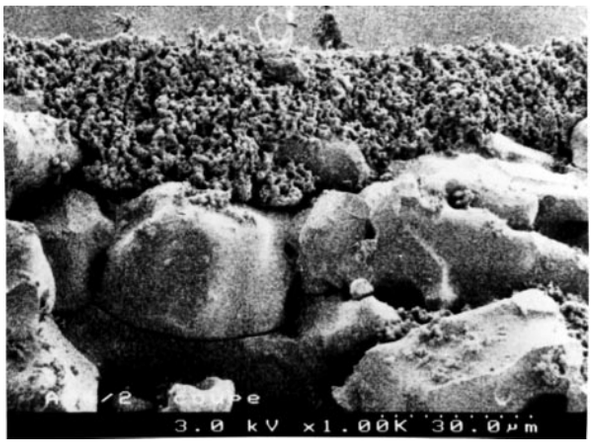

Fig. 7 SEM microphotograph of the cross-section of sample 7.

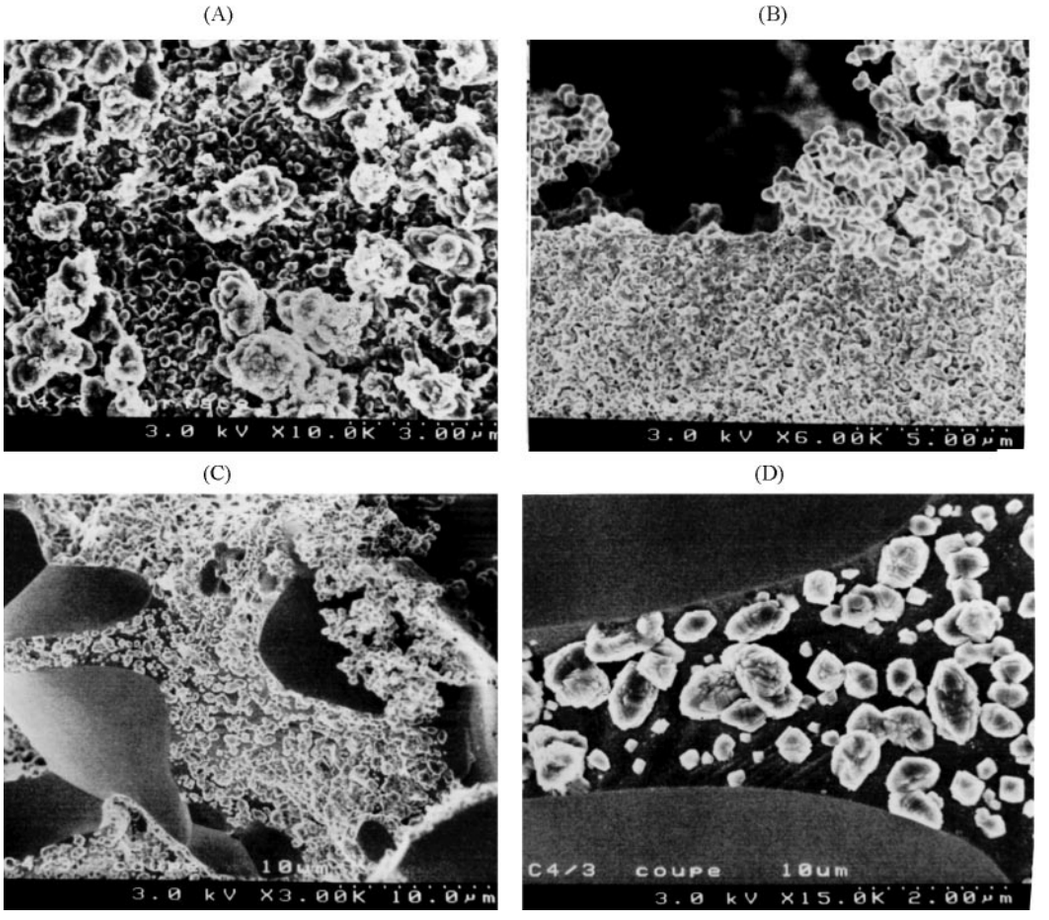

Fig. 8 SEM microphotographs of sample 11: (A) top surface, (B) cross-section and (C and D) macroporous layers of the support.

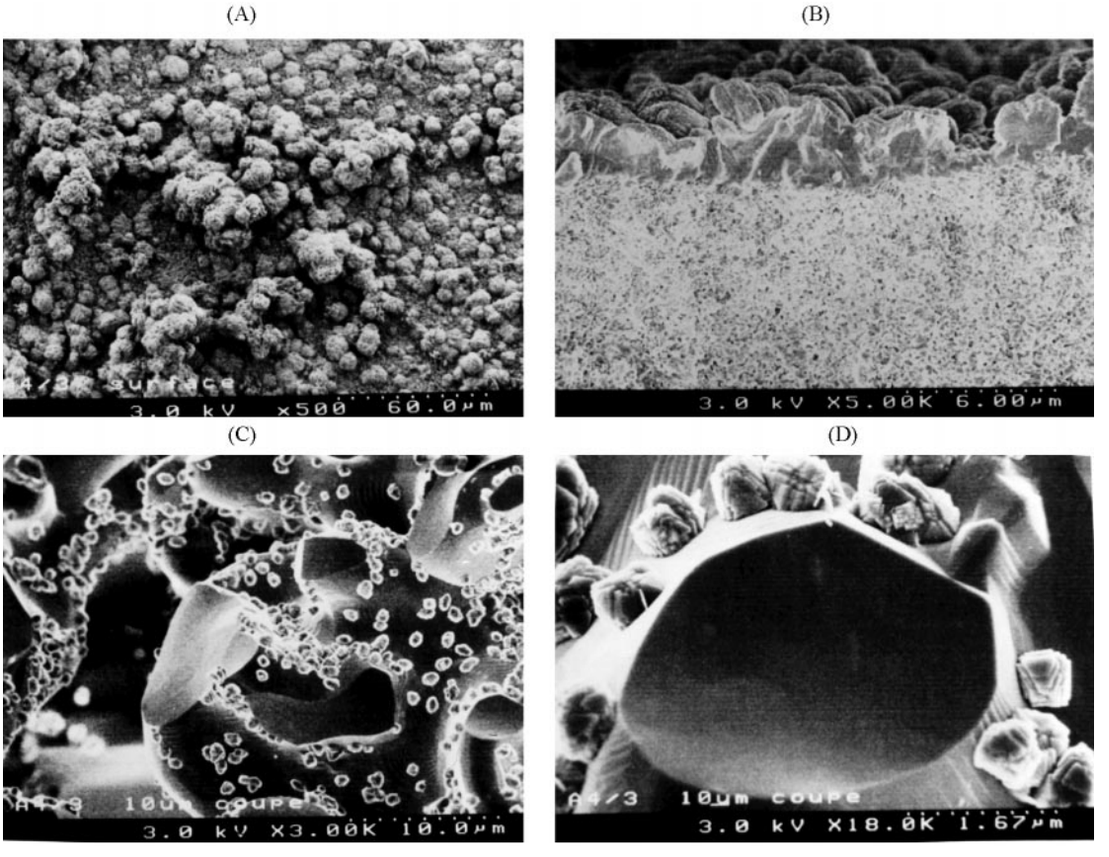

Fig. 9 SEM microphotographs of sample 10: (A) top surface, (B) cross-section and (C and D) macroporous layers of the support.

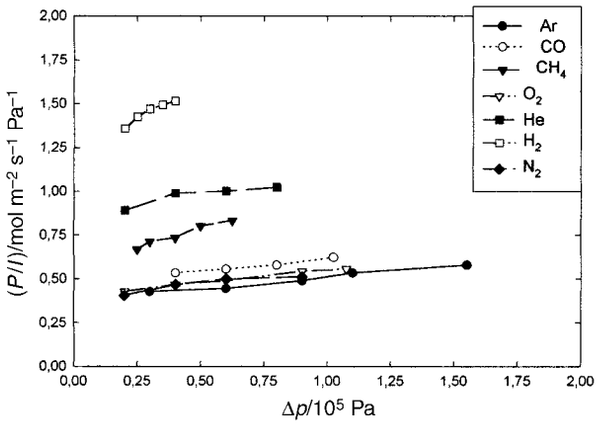

Fig. 10 Evolution of single gas permeances as a function of the transmembrane pressure through the MOR membrane, at 294 K.

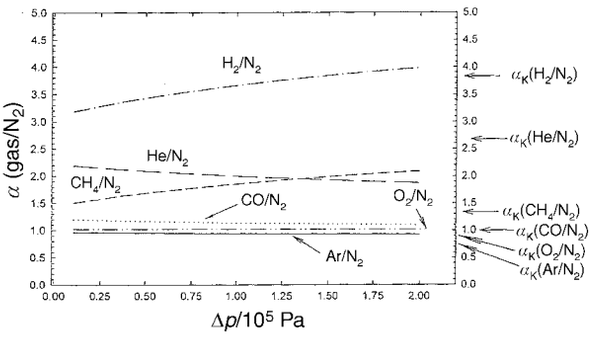

Fig. 11 Evolution of the ideal selectivity of the MOR membrane as a function of the transmembrane pressure at 294 K.

with caution ($1.0\ \mathrm{K\ min^{-1}}$) because the different thermal expansion coefficients of the membrane materials can induce the formation of defects. The permeances of pure gas through the resulting membrane are shown in Fig. 10 at 294 K as a function of the transmembrane pressure (Δp). The permeances of N_2, O_2, Ar, CO, He and CH_4 slightly depend on Δp, although the H_2 permeance is more strongly influenced by Δp in the range $0.5\times10^5\ \mathrm{Pa} < \Delta p < 0.4\times10^5\ \mathrm{Pa}$. The evidence of a small viscous flow contribution demonstrates that the membrane contains a small number of macrodefects, which also contribute to gas transport. The macrodefects, initially not observed, might have been generated during the calcination procedure by template removal, thereby inducing a certain viscous flow contribution.

Table 2 reports the experimental permeance ratios of the various gases with respect to nitrogen for the MOR composite membrane. The Knudsen selectivities and data found in the literature for different zeolite structures[16] are also reported for comparison. The measured permeance values (from 4 to $15\times10^{-7}\ \mathrm{mol\ s^{-1}\ Pa^{-1}\ m^{-2}}$) are typically in the range of those reported in the literature for zeolite membranes. The experimental permeance ratios of the MOR membrane, calculated for $\Delta p = 0.4\times10^5$ Pa and $T = 294$ K, are close to the Knudsen selectivities. The permeance ratios of the various gases with respect to N_2 are reported in Fig. 11 as a function of Δp, together with the Knudsen selectivity values. The experimental permeance ratios for Ar/N_2, O_2/N_2 and CO/N_2 are close to

Table 2 Gas permeances and separation factors of zeolite composite membranes

Zeolite type	Support	T/K	Permeance/10^7 mol^{-1} m^{-2} Pa^{-1}	Permeance ratio P_i/P_{N_2}	Knudsen selectivity	Reference
MOR	α-Al_2O_3	294	H_2 = 15.15 N_2 = 4.68 Ar = 4.46 O_2 = 4.68 CO = 5.35 He = 9.89 CH_4 = 7.35	H_2/N_2 = 3.23 Ar/N_2 = = 0.89 O_2/N_2 = 1.00 CO/N_2 = 1.14 He/N_2 = 2.11 CH_4/N_2 = 1.57	H_2/N_2 = 3.73 Ar/N_2 = 0.84 O_2/N_2 = 0.93 CO/N_2 = 1.00 He/N_2 = 2.64 CH_4/N_2 = 1.32	This work
A	α-Al_2O_3	308	H_2 = 10.0 N_2 = 1.0 O_2 = 2.0 CO_2 = 10.0 He = 6.0 CH_4 = 9.0	H_2/N_2 = 9.4; 4.8 He/CO_2 = 9.0		10
Silicalite	Stainless steel	673	H_2 = 2.50 N_2 = 15.0 Ar = 2.0 CO = 15.0 CH_4 = 4.0	H_2/N_2 = 0.17 Ar/N_2 = 0.13 CO/N_2 = 1.0 CH_4/N_2 = 0.27		11
MFI	α-Al_2O_3	303	N_2 = 0.32 CO_2 = 1.05 He = 0.6 CH_4 = 0.8	CO_2/N_2 = 3.28 He/N_2 = 1.87 CH_4/N_2 = = 2.5		12
Silicalite	α-Al_2O_3	298	H_2 = 1.3 Ar = 0.8 N_2 = 0.8	H_2/N_2 = 1.67 Ar/N_2 = 1.00		13
ZSM-5	α-Al_2O_3	300	H_2 = 1.25 N_2 = 0.32 O_2 = 0.46 CO_2 = 0.51 He = 1.03	H_2/N_2 = 3.91 He/N_2 = 3.22 O_2/N_2 = 1.45 CO_2/N_2 = 1.6		14
ZSM-5	γ-Al_2O_3	300	H_2 = 44 N_2 = 15.6 He = 26.7	H_2/N_2 = 2.8 He/N_2 = 1.7		15
MOR	Al_2O_3	294	H_2 = 8.4 N_2 = 3.5 O_2 = 2.9 CO_2 = 2.5 He = 5.5 CH_4 = 3.2	H_2/N_2 = 2.4 O_2/N_2 = 0.83 He/N_2 = 1.57 CH_4/N_2 = 0.9		16

Knudsen selectivity. On the other hand the experimental permeance ratio for CH_4/N_2 is slightly higher than the Knudsen selectivity, although it is lower for He/N_2 and lower or equal for H_2/N_2. It should be noted that the membrane ideal selectivity was found to be sensitive to Δp only in the cases of H_2/N_2, He/N_2 and CH_4/N_2. This type of behaviour should be due to the differential adsorption effects on the MOR membrane material.

The evolution of MOR membrane permeance at 294 K and $\Delta p = 0.4 \times 10^5$ Pa is reported in Fig. 12 as a function of the gas kinetic diameters. The results obtained by Aoki *et al.*[10] and by Bakker *et al.*,[11] respectively, for an A-type zeolite membrane and for a silicalite-1 membrane are also reported for comparison. A similar trend is observed for the three types of membrane in spite of the highly exacerbated CH_4 permeance observed for the silicalite membrane. The behaviors of the A-type and MOR membranes are much more similar except that the order of gas permeance slightly differs for O_2, N_2 and CH_4 ($O_2 \simeq N_2 < CH_4$ for MOR and $O_2 \simeq CH_4 > N_2$ for the A membrane). MOR membrane leads to a lower O_2/N_2 and higher CH_4/N_2 ideal selectivities compared to the A-type zeolite membrane.

The evolution of the permeance as a function of the inverse square root of the molecular weight ($M^{-1/2}$) suggests that Knudsen diffusion is the dominant transport mechanism for the investigated series of gases for both the A-type and the MOR-type membranes. *Vice versa* the silicalite membrane does not obey the Knudsen diffusion mechanism. This conclusion was already mentioned in the case of the silicalite membrane by Bakker *et al.*[11] for H_2 and He at 303 K and for the other gases at 673 K when adsorption no longer dominated gas transport. Further permeation studies with CO_2, with heavier alkanes and at high temperature, coupled with adsorption measurements, will be necessary to better evaluate membrane performance.

The overall results show that we have obtained a MOR microporous system.

Conclusions

A MOR composite membrane was synthesized on porous tubular α-alumina supports by hydrothermal treatment. The influence of several synthesis parameters (temperature, pH, role of TEA^+, and silica source) were studied in order to obtain a MOR composite membrane with intergrown crystals both on the surface and in the porous layers of the alumina support. The optimal starting composition of nutrients was: $5.7Na_2O$–Al_2O_3–$30SiO_2$–$3.0TEAOH$–$1500H_2O$ and the hydrothermal synthesis was performed at 423 K. The single gas permeation studies performed at room temperature revealed a small viscous flow contribution for gas transport through the MOR composite membrane. Furthermore, these preliminary results (order of gas permeance and ideal selectivity) suggest that Knudsen diffusion is the dominant transport mechanism for the investigated series of gases (H_2, N_2, O_2, Ar, CO, He and CH_4), although a selectivity higher than the Knudsen one was obtained namely for CH_4/N_2. In order to better characterize the gas transport mechanisms through this type of MOR composite membrane, further permeation studies, with CO_2, with heavier alkanes and at higher temperatures, are being currently investigated. Membrane synthesis reproducibility and the insertion of noble metals (by ionic exchange) will be also studied.

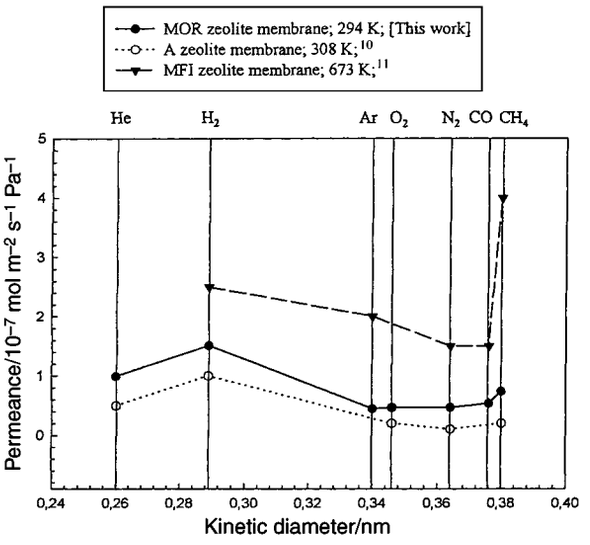

Fig. 12 Evolution of the single gas permeances as a function of the gas kinetic diameters for MOR [this work], silicalite-1[11] and A-type[10] zeolite membranes. The temperature is in the range 294–308 K.

Acknowledgements

This work was supported both by Regione Calabria (Programma Operativo Plurifondo 1994/1999; Sottoprogramma 4; Misura 4,4 "Ricerca Scientifica e Tecnologica") and by the agreement with the CNR-CNRS (Project N° 3183). The authors wish to express their sincere thanks to Didier Cot and Georges Nabias (LMPM-Montpellier-France) for SEM observations.

References

1 A. Tavolaro and E. Drioli, *Adv. Mater.*, 1999, **12**, 975.
2 Z. A. E. P. Vroon, K. Keizer, A. J. Burgraaf and H. Verweij, *J. Membr. Sci.*, 1998, **144**, 65.
3 C. S. Brooks, *Adv. Chem. Ser.*, 1971, **102**, 406.
4 J. N. Miale and P. B. Weisz, *J. Catal.*, 1971, **20**, 288.
5 K. A. Brecker, H. G. Karge and W. D. Streubel, *J. Catal.*, 1973, **28**, 403.
6 A. N. Keough and L. B. Sand, *J. Am. Chem. Soc.*, 1961, **83**, 3536.
7 N. Nishiyama, K. Ueyama and M. Matsukata, *Microporous Mater.*, 1996, **1**, 299.
8 M. Matsukata, N. Nishiyama and K. Ueyama, *Stud. Surf. Sci. Catal.*, 1994, **84B**, 1183.
9 M. L. Sand, W. S. Colblenz and L. B. Sand, *Molecular Sieve Zeolites*, *Adv. Chem. Ser.*, ACS, Washington DC, 1971, p. 127.
10 A. Aoki, K. Kusakabe and S. Morooka, *J. Membr. Sci.*, 1998, **141**, 197.
11 W. J. W. Bakker, L. J. P. Van der Broeke, F. Kapteijn and J. A. Moulijn, *AIChE J.*, 1997, **9**, 2203.
12 K. Kusakabe, S. Yoneshige, A. Murata and S. Morooka, *J. Membr. Sci.*, 1996, **116**, 39.
13 X. Xu, M. Cheng, W. Yang and L. Lin, *Sci. China, Ser. B*, 1998, **41**(3), 325.
14 H.-S. Oh, M. H. Kim and H. K. Rhee, *Stud. Surf. Sci. Catal.*, 1997, **105**, 2217.
15 M.-D. Jia, B. Chen, R. D. Noble and J. L. Falconer, *J. Membr. Sci.*, 1994, **90**, 1.
16 N. Nishiyama, K. Ueyama and M. Matsukata, *AIChE J.*, 1997, **11A**, 2724.